J. Phys.: Condens. Matter **21** (2009) 025505 (7pp) doi:10.1088/0953-8984/21/2/025505

First-principles calculations of elastic and electronic properties of NbB_2 under pressure

Xiao-Feng Li[1,2], Guang-Fu Ji[1,2,5], Feng Zhao[2], Xiang-Rong Chen[1,3,5] and Dario Alfè[4]

[1] School of Physical Science and Technology, Sichuan University, Chengdu 610064, People's Republic of China
[2] Laboratory for Shockwave and Detonation Physics, Institute of Fluid Physics, China Academy of Engineering Physics, Mianyang 621900, People's Republic of China
[3] International Centre for Materials Physics, Chinese Academy of Sciences, Shenyang 110016, People's Republic of China
[4] Department of Physics and Astronomy, University College London, Gower Street, London WC1E 6BT, UK

E-mail: cyfjkf@caep.ac.cn and xrchen@scu.edu.cn

Received 1 July 2008, in final form 11 November 2008
Published 10 December 2008
Online at stacks.iop.org/JPhysCM/21/025505

Abstract

The structural parameters, elastic constants and electronic structure of NbB_2 under pressure are investigated by using first-principles plane-wave pseudopotential density functional theory within the generalized gradient approximation (GGA). The obtained results are in agreement with the available theoretical data. It is found that the elastic constants and the Debye temperature of NbB_2 increase monotonically and the anisotropies weaken with pressure. The band structure and density of states (DOS) of NbB_2 under pressure are also presented. It is the σ hole that determines the superconductivity in NbB_2, and the features of the σ bands are unchanged after applying pressure except for a shift of position. The density of states (DOS) at the Fermi level decreases with increasing pressure, in conjunction with Bardeen–Cooper–Schrieffer (BCS) theory, which can predict T_c decreasing with pressure, in agreement with the trend of the theoretical T_c versus pressure.

1. Introduction

Since the discovery of superconductivity at $T_c = 39$ K in MgB_2 [1], the physical properties of the group V transition metal diborides with simple hexagonal AlB_2-type structure have attracted significant interest. In particular, the diborides of transition metals observed by Buzea *et al* [2] are not superconducting except for NbB_2. Hexagonal NbB_2 (space group $P6/mmm$, $a = 3.116$ Å, $c = 3.264$ Å [3]) has been reported to show superconductivity, $T_c = 3.87$ K [4]. The transition temperature T_c in $Nb_{1-x}B_2$ ($0 < x < 1$) increases to around 9 K, especially in Nb-deficient samples, though NbB_2 did not show superconductivity at $T < 1.8$ K [5]. A series of studies [6–10] confirmed these results; in particular, the highest $T_c \sim 9.8$ K was observed in $Nb_{1-x}B_2$(B/Nb = 2.34) [7].

[5] Authors to whom any correspondence should be addressed.

Due to a great deal of attention on NbB_2, several research groups have investigated the physical properties of NbB_2. Islam *et al* [11, 12] studied the zero-pressure elastic constants and electronic structure of NbB_2 using *ab initio* density functional theory and found that the superconducting transition temperature decreases under pressure. Using the full-potential linearized augmented plane-wave (FP-LAPW) method, the influence of lattice vacancies on the structural, cohesive, and electronic properties of Nb and Mo diborides were obtained by Shein *et al* [13]. With the full-potential density-functional-based methods, Singh [14] investigated the significant differences in electron–phonon interaction of MgB_2 and NbB_2, which lead to the distinction of their superconducting transition temperatures. The electronic structure and structure equilibrium parameters of some AlB_2 type transition metal diborides were calculated by Vajeeston *et al* [15]

Table 1. Calculated structure parameters of NbB_2 compared with the experimental and theoretical results at 0 GPa and 0 K.

	a (Å)	c (Å)	V (Å^3)	B_0 (GPa)	B'	r_{Nb-B}	r_{B-B}
Present	3.1136	3.3066	27.8	294.9	3.99	2.442	1.798
Reference [11]	3.1598	3.4003	29.4	232.4	3.60	2.488	1.820
Reference [13]	3.1110	3.3086	27.7			2.4416	1.7959
Reference [14]	3.0745	3.2280	26.4				
Reference [15]	3.1070	3.3180	27.8			2.447	1.794
Reference [16]	3.093	3.337	27.3			2.477	1.794
Exp. [3]	3.116	3.264	27.4				
Exp. [14]	3.089	3.3047	27.3				

using the self-consistent tight-binding linear muffin-tin orbital method. The phonon density of states of transition metal diborides TMB_2 (TM = Ti, V, Ta, Nb, and Y) has been measured using the technique of inelastic neutron scattering [16].

Elastic properties of a solid are closely correlated with various fundamental physical properties, such as specific heat, melting point, interatomic bonding, equation of states, Debye temperature, thermal expansion coefficient, and so on. Moreover, what is more important, the knowledge of elastic constants of a solid provides access to understand the mechanical properties for practical application in many fields, e.g. sound velocity, anisotropy, thermoelastic stress, load deflection, fracture toughness, etc. Furthermore, one can also directly obtain some useful information on the characteristics of bonding and the structural stability of a crystal.

However, previous work by others [11–16] only addressed the structural properties and electronic structure of NbB_2 at zero pressure. It is known that pressure is an important parameter to tune physical properties, so it attracts us to investigate the elastic and electronic properties of NbB_2 under pressure. To our knowledge, for the two superconductor diborides (NbB_2 and MgB_2), only elastic constants [17, 18], anisotropies and the electronic structure of MgB_2 under pressure have been computed successfully; there are few investigations on the properties of NbB_2 under pressure. In this work, we investigate elastic properties and electronic structure of NbB_2 under pressure using the first-principles plane-wave method within the generalized gradient approximation (GGA).

2. Computational method

In this work, we focus on elastic properties and electronic band structure of NbB_2 under high pressures using the plane-wave pseudopotential density functional theory method. Here we employ non-local ultrasoft pseudopotentials introduced by Vanderbilt [19], together with the Perdew–Burke–Ernzerhof (PBE) generalized gradient approximation (GGA) exchange–correlation functional [20]. The electronic wavefunctions are expanded in a plane-wave basis set with energy cut-off 400.0 eV. Pseudoatomic calculations are performed for Nb $4s^2 4p^6 4d^4 5s^1$ and B $2s^2 2p^1$. As for the Brillouin-zone sampling, we use the Monkhorst–Pack mesh with $12 \times 12 \times 12$ k-points, where the self-consistent convergence of the total energy is set to 10^{-6} eV/atom. These parameters are sufficient in leading to well converged total energy. All the electronic structure calculations are implemented through the CASTEP code [21, 22].

3. Results and discussion

3.1. Structure properties

The total energy electronic structure calculations are performed over a range of primitive cell volume V from 0.82 V_0 to 1.10 V_0, in which V_0 is the zero pressure equilibrium primitive cell volume. No constraints are imposed on the c/a ratio, i.e. the lattice constants a and c are optimized simultaneously. For each volume, we determine the corresponding equilibrium ratio c/a of NbB_2 by performing total energy calculations on a series of different c/a ratios and minimize the energy as function of c/a. Through these calculations, we can obtain the equilibrium parameters a and c and the corresponding equilibrium ratio c/a of NbB_2 under arbitrary pressures. The calculated equilibrium lattice parameters are listed in table 1, together with other theoretical [11–16] and experimental [3, 14] data. The zero pressure bulk modulus B_0 and the derivative of the bulk modulus with respect to pressure B_0' are obtained from the Birch–Murnaghan equation of state (EOS) [23], and are also shown in table 1. It is clear that our results are in good agreement with the experimental data and other theoretical results.

In figure 1(a), we exhibit the dependence on pressure of the normalized lattice parameters c/a, a/a_0, and c/c_0 as well as the normalized volume V/V_0 (where a_0, c_0, and V_0 are the zero pressure equilibrium structure parameters). Unfortunately, there are few experimental data to compare with. The normalized intermolecular distances r_1/r_{10} and r_2/r_{20} (where r_{10} and r_{20} are the zero pressure equilibrium distances of Nb–B and B–B, respectively) are shown in figure 1(b). We notice in figure 1(a) that, when pressure increases, the equilibrium ratio c/a ranges from 1.081 at −30 GPa to 1.049 at 80 GPa, i.e. decreases by about 2.96%; the compression along the c-axis is much larger than that along the a-axis in the basal plane. Figure 1(b) indicates that the curve of r_1/r_{10} (the distance between the Nb atom and the B atom) becomes steeper as pressure increases, indicating that the direction along Nb–B is compressed more easily. These results agree with weaker Nb–B bonds that determine the lattice parameter c. Moreover, the atoms in the interlayers become closer, and the interactions between them become stronger; contraction of Nb–B and B–B interatomic distances

Table 2. Elastic constants C_{ij} (GPa) and the bulk moduli B_a and B_c (GPa) at 0 GPa and 0 K.

	C_{11}	C_{12}	C_{13}	C_{33}	C_{44}	B_a	B_c
Present work	576	114	198	430	210	940	742
References [11, 12] (NbB_2)	517	95	120	528	122	797	557
Reference [17] (MgB_2)	462	67	41	254	80	615	293
Reference [28] (VB_2)	699	146	109	552	167	999	706
Reference [28] (ZrB_2)	596	48	169	482	240	809	828
Exp. [29] (ZrB_2)	568	57	121	436	248	772[a]	635[a]
Exp. [30] (TiB_2)	660	48	93	432	260	851[a]	553[a]

[a] Derived from the experimental elastic constants.

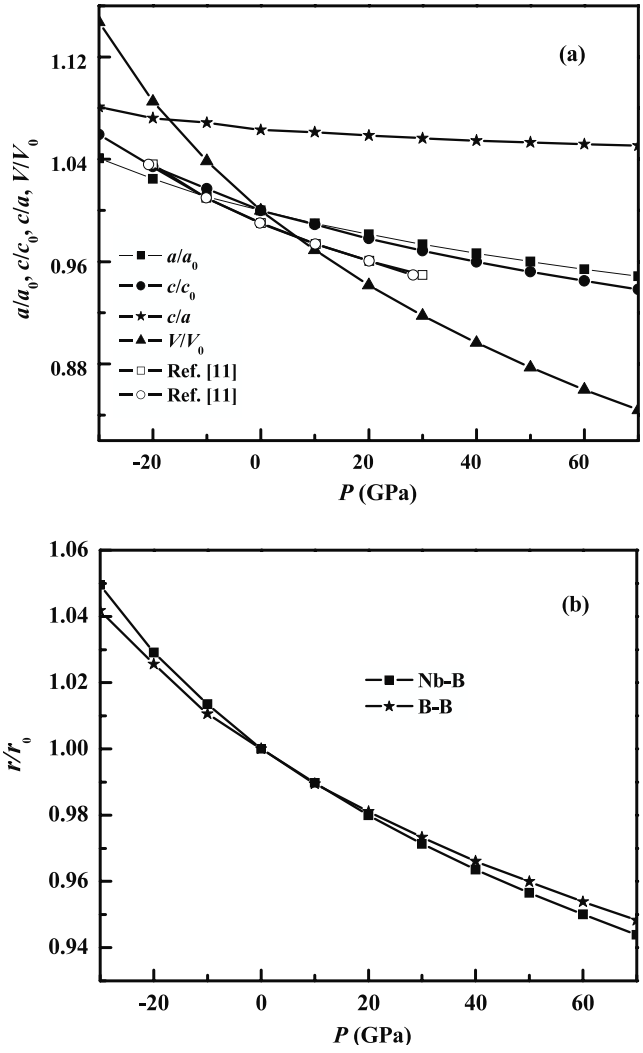

Figure 1. (a) The normalized volume V/V_0, a/a_0, c/c_0, and c/a as a function of pressure at $T = 0$, where the rectangles, circles, and triangles represent our obtained V/V_0, a/a_0, and c/c_0 respectively, and the blank ones are the results from [11]; (b) variation of the normalized distance r/r_0 between the atoms with pressure.

under pressure results in the change of bonding anisotropy of NbB_2 structure, which induces the variety of electronic structure. The interlayer linear compressibility ($\mathrm{d}\ln c/\mathrm{d}p = 0.001\,46$ GPa^{-1}) is about 1.38 times larger than that in the basal plane ($\mathrm{d}\ln a/\mathrm{d}\ln p = 0.001\,09$ GPa^{-1}), in which B–B bonds are covalent.

3.2. Elastic properties and anisotropies under pressure

To calculate the elastic constants under pressure, we have applied the non-volume-conserving method. The complete elastic constant tensor was determined from calculations of the stresses induced by small deformations of the equilibrium primitive cell, and thus the elastic constants C_{ijkl} are determined as [24–26]

$$c_{ijkl} = \left(\frac{\partial\sigma_{ij}(x)}{\partial e_{kl}}\right)_X \tag{1}$$

where s_{ij} and e_{kl} are the applied stress and Eulerian strain tensors, and X and x are the coordinates before and after the deformation. For the isotropic stress, the elastic constants are defined as [25–27]

$$c_{ijkl} = C_{ijkl} + \frac{P}{2}(2\delta_{ij}\delta_{kl} - \delta_{il}\delta_{jk} - \delta_{ik}\delta_{jl}) \tag{2}$$

$$C_{ijkl} = \left(\frac{1}{V(x)}\frac{\partial^2 E(x)}{\partial e_{ij}\partial e_{kl}}\right)_X \tag{3}$$

where C_{ijkl} are the second-order derivatives with respect to the infinitesimal strain (Eulerian). For hexagonal crystals, there are five independent elastic constants.

We have calculated the five independent elastic constants of NbB_2 using the stress–strain relation. In table 2, we list the elastic constants of NbB_2 at 0 K and 0 GPa. It is shown that the differences between our results and Islam *et al* [11, 12] are a bit large. Since there are no experimental data to compare with, we here thus list the results of other similar types of diborides. The lattice parameters listed in table 1 from our calculations seem to be better than those by Islam *et al*, and we think that our calculations for elastic constants should be reliable.

The mechanical anisotropy of NbB_2 can be calculated using the bulk moduli along the a and c axes, B_a and B_c respectively, defined as

$$B_a = a\frac{\mathrm{d}p}{\mathrm{d}a} = \frac{\Lambda}{2+\alpha}, \tag{4}$$

$$B_c = c\frac{\mathrm{d}p}{\mathrm{d}c} = \frac{B_a}{\alpha}, \tag{5}$$

$$\Lambda = 2(C_{11} + C_{12}) + 4C_{13}\alpha + C_{33}\alpha^2, \tag{6}$$

$$\alpha = \frac{C_{11} + C_{12} - 2C_{13}}{C_{33} - C_{13}}. \tag{7}$$

The calculated B_a and B_c at zero pressure are also presented in table 2, together with results of others. The ratio

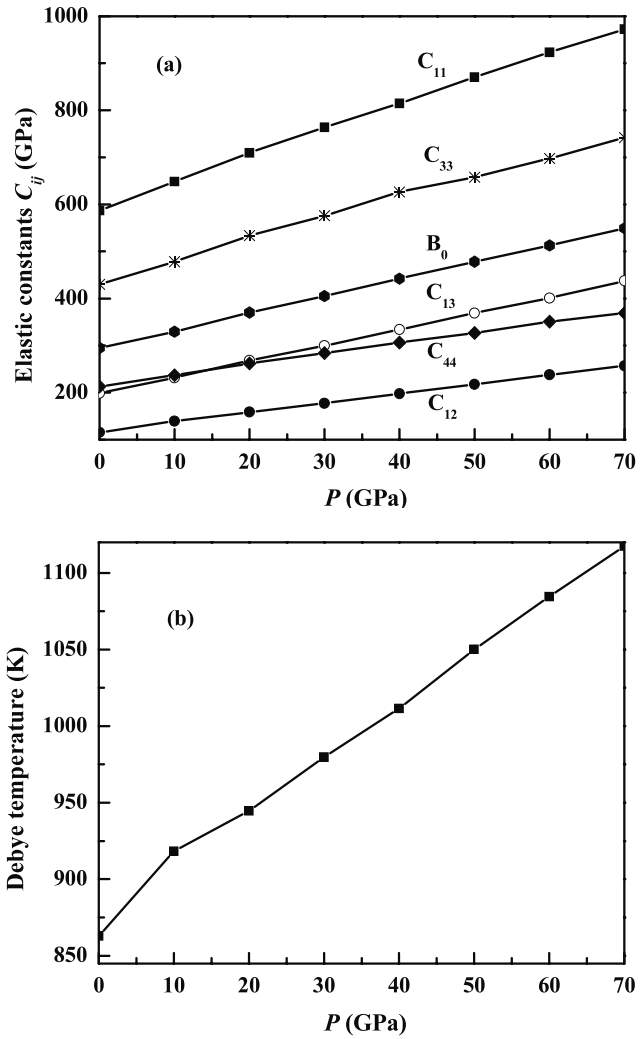

Figure 2. (a) The elastic constants C_{ij} and the bulk modulus B_0 as a function of pressure of NbB_2; (b) variations of the Debye temperature Θ_D dependences on pressure.

B_a/B_c of NbB_2 is 1.27 (2.10 for MgB_2 [17], 1.54 for TiB_2 [30], 1.42 for VB_2 [28], 0.98 [28] and 1.22 [29] for ZrB_2), which is in agreement with the value of 1.43 presented by Islam *et al*. The ratio B_a/B_c of NbB_2 is smaller than MgB_2, TiB_2 and VB_2, indicating the stronger interaction for NbB_2. But in comparison to ZrB_2, the interaction of NbB_2 is weaker.

The obtained values of C_{11}, C_{12}, C_{13}, C_{33}, C_{44}, and B_0 at zero temperature versus pressure (up to 70 GPa) are shown in figure 2. We found that the five independent elastic constants and the bulk modulus B_0 increase monotonically with pressure. C_{11} and C_{33} vary rapidly as pressure increases, and C_{12} becomes moderate as well as C_{13}. However, C_{44} increases comparatively slowly with pressure. Unfortunately, there are no experimental and theoretical data to compare our elastic constants under pressure.

It is known that the acoustic velocities are obtained from elastic constants by the Christoffel equation [31]

$$(C_{ijkl}n_jn_k - M\delta_{il})\mu_i = 0 \tag{8}$$

where $M = \rho v^2$, C_{ijkl} is the fourth rank tensor description of the elastic constants, n is the propagation direction, and μ is the polarization vector; the acoustic anisotropy is defined as [32]

$$\Delta_i = \frac{M_i[n_x]}{M_i[100]} \tag{9}$$

where n_x is the extremal propagation direction and i is the index of three types of elastic waves (one longitudinal and two traversal polarizations of shear waves). By solving the Christoffel equation (8) for hexagonal NbB_2, the anisotropy of the compressional wave is obtained from

$$\Delta_P = \frac{C_{33}}{C_{11}}. \tag{10}$$

The anisotropies of the wave polarized perpendicular to the basal plane ($S1$) and the polarized basal plane ($S2$) are calculated

$$\Delta_{S1} = \frac{C_{11} + C_{33} - 2C_{13}}{4C_{44}}, \qquad \Delta_{S2} = \frac{2C_{44}}{C_{11} - C_{12}}. \tag{11}$$

The calculated pressure dependences of the anisotropies Δ_p, Δ_{S1} and Δ_{S2} for the three types of elastic waves in NbB_2 are illustrated in figure 3. It is noted that with increasing pressure Δ_p and Δ_{S2} increase but only slightly. However, Δ_{S1} decreases sharply with pressure (due to the fact that the elastic constants C_{11} and C_{33} are affected by pressure). The anisotropy is only dependent on the symmetry of the crystal. The structure of the crystal has been changed under applied pressures because of the variations of c/a at various pressures. Therefore, the elastic anisotropy is different due to the variations of the elastic constants with pressure. This also corresponds to the stronger covalent bonding in boron layers, ionized magnesium atoms and weaker interlayer metallic bonding for NbB_2.

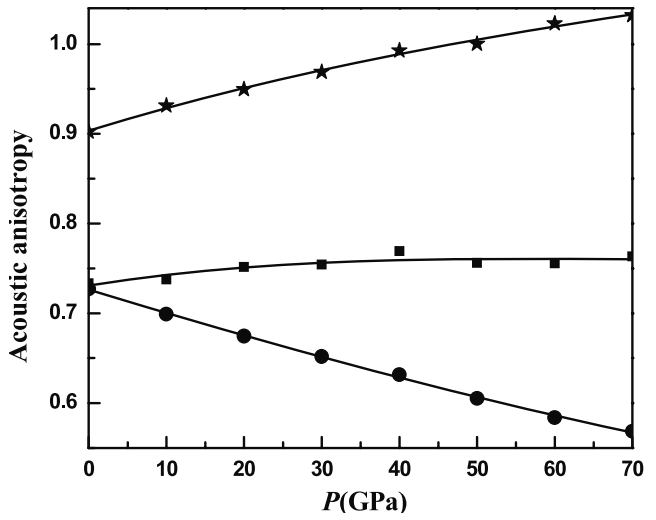

Figure 3. The anisotropies, elastic constant ratios C_{33}/C_{11}, $(C_{11} + C_{33} - 2C_{13})/4C_{44}$, $2C_{44}/(C_{11} - C_{12})$, which can determine the anisotropies of the compressional wave (Δ_P) and the shear wave (Δ_{S1} and Δ_{S2}), are displayed as functions of various pressures. The squares, circles and stars represent Δ_P, Δ_{S1} and Δ_{S2}, respectively.

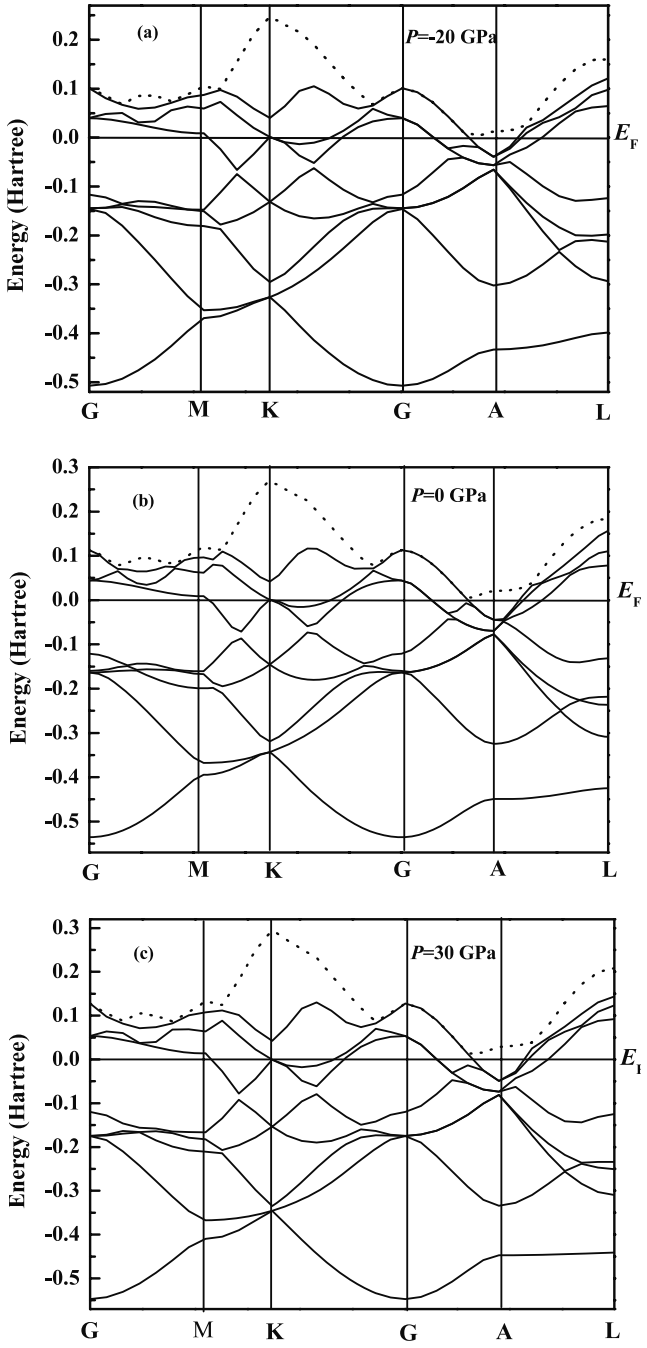

Figure 4. Band structure of NbB_2 at pressure (a) −20 GPa, (b) 0 GPa, and (c) 30 GPa, where the dotted line represents the π band.

3.3. Thermodynamic properties

As an important physical quantity, the Debye temperature is closely related to the elastic constants, specific heat and melting point. The vibrational excitations at low temperatures arise solely from acoustic vibrations. So at low temperatures the Debye temperature obtained from elastic constants is the same as that determined from specific heat measurements. One popular method to calculate the Debye temperature Θ_D is from elastic constants, i.e. Θ_D is estimated from the average sound velocity v_m, via the following equation [33]:

$$\Theta_D = \frac{h}{k}\left[\frac{3n}{4\pi}\left(\frac{N_A\rho}{M}\right)\right]^{\frac{1}{3}} v_m \tag{12}$$

where h is the Planck's constant, k is the Boltzmann's constant, N_A is the Avogadro's number, n is the number of atoms in the molecule, M is the molecular weight, and ρ is the density. The average wave velocity v_m is approximately calculated from

$$v_m = \left[\frac{1}{3}\left(\frac{2}{v_s^3} + \frac{1}{v_p^3}\right)\right]^{-\frac{1}{3}} \tag{13}$$

where v_p and v_s are the compressional and shear wave velocity, respectively, which are obtained from the Navier's equation [34]:

$$v_p = \sqrt{\left(B + \tfrac{4}{3}G\right)/\rho}, \qquad v_s = \sqrt{G/\rho} \tag{14}$$

where G is the shear modulus. The Debye temperatures Θ_D of NbB_2 are also exhibited at various pressures in figure 2(b). At $P = 0$ GPa and $T = 0$ K, $\Theta_D = 862.9$ K, which is higher than the theoretical value of 753.3 K calculated from the elastic constants by Islam *et al* [11, 12]. Our calculated value is close to those of TiB_2 (970 K), VB_2 (1038 K), ZrB_2 (931 K) [28], and MgB_2 (819 K) [35], which are also derived from elastic constants. From figure 2(b), it is shown that the Debye temperature increases monotonically with increasing pressure.

3.4. Electronic structure of NbB_2 under pressure

Finally, the effects of pressure on the band structure and the density of states (DOS) of NbB_2 are examined, where pressure varies in the range from −20 to 30 GPa. The band structure near the Fermi level at $P = 0$ GPa is shown in figure 4(b). There are general features of the band structure which are in good agreement with other studies [11, 13]. The two notable types of band are the σ and π bands, which are formed by the hybridizations of Nb d states, B s states and B p states. In figure 4, above the Fermi level, the dotted line is the π band, and the solid lines represent the σ band. The σ band along the G–A line is doubly degenerate and makes a large contribution to the DOS at the Fermi level. The band structures under pressure along the symmetry directions are exhibited in figures 4(a) and (c). Although there is a shift of position under pressure, the dispersion increases only slightly. Due to the maintaining of the symmetry of NbB_2, the features of the σ bands are hardly changed after applying pressure on NbB_2. Figure 5 displays the pressure dependence of the total and partial density of states of NbB_2 near the Fermi level, where the vertical line is the Fermi level E_F. The calculated equilibrium density of states at the Fermi level E_F ($P = 0$ GPa) is 27.6 states/Hartree, which is in agreement with those of other works [11, 13, 15]. The partial densities of states (DOSs) of the s, p, and d electrons of Nb and the s and p electrons of B at $P = 0$ are exhibited in figure 6. The features are depicted as follows: there are high DOSs near the Fermi level;

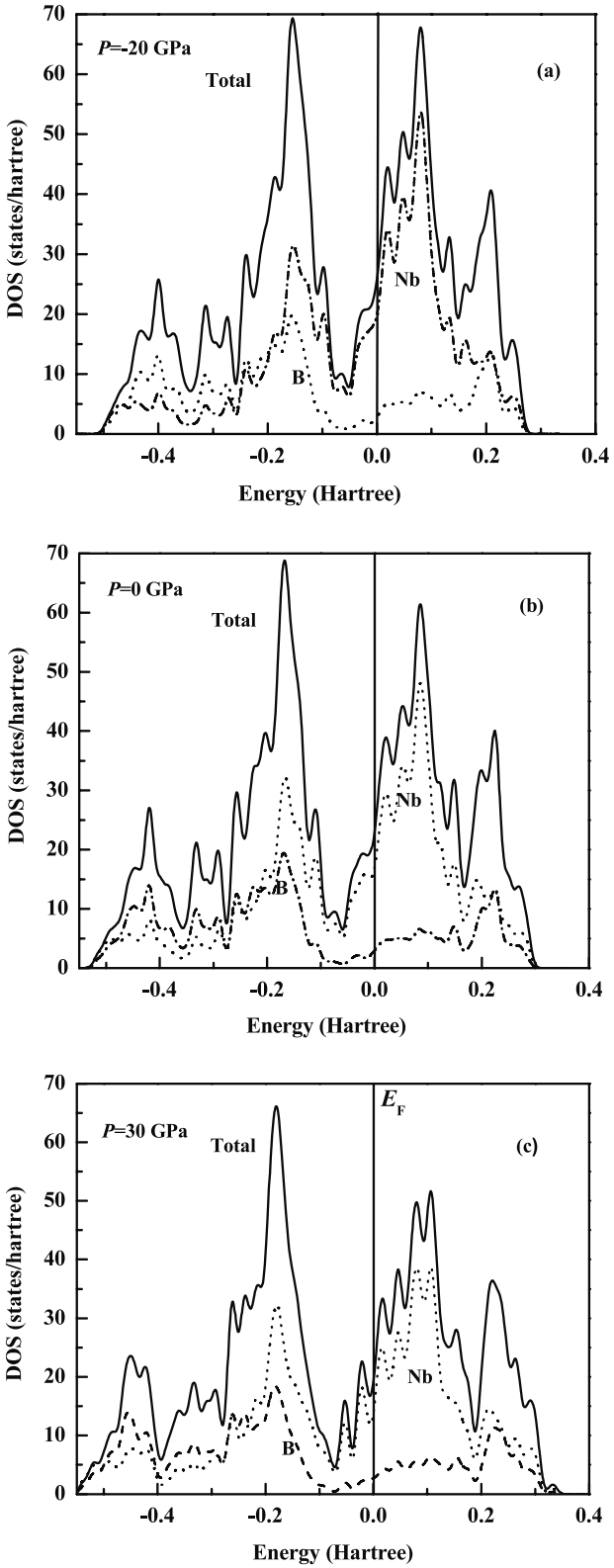

Figure 5. The total and partial DOS of NbB_2 under pressure (a) −20 GPa, (b) 0 GPa, and (c) 30 GPa.

moreover, the B p states and Nb d states contribute more to the DOS at the Fermi level (figure 6). The value of the DOS at E_F reduces to 19.2 states/Hartree at $P = 30$ GPa. The value of the DOS at E_F decreases by as much as about

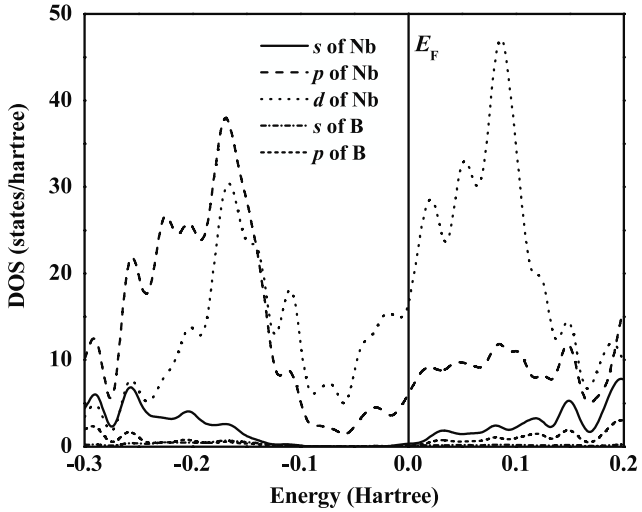

Figure 6. The partial DOS of s, p and d electrons of Nb and s and p electrons of B at $P = 0$ Gpa.

30.5% as pressures vary from 0 to 30 GPa. This behavior is similar to that observed in MgB_2 [18]. The presences of the sharp peaks are due to the covalent hybridization of Nb and B atoms; their hybridization energy decreases with pressure. The DOS at the Fermi level is an important parameter known to affect the superconducting transition temperature T_c. Judging from Bardeen–Cooper–Schrieffer superconducting theory, the reducing density of states at the Fermi level [36] shows that the transition temperature T_c decreases as pressures increase, which is consistent with the T_c–P relation obtained by Islam *et al* [11].

4. Conclusion

In summary, we have focused our attention on the elastic constants and the anisotropy as well as the density of states (DOS) under high pressures by using plane-wave pseudopotential density functional theory within the generalized gradient approximation (GGA). We have obtained the pressure dependence of structural parameters $a, c, c/a, V$ and r (the distance of Nb–B, B–B) through performing total energy calculations over a range of the primitive cell volumes. The results are in agreement with other theoretical data. The pressure dependences of elastic constants and bulk modulus are also obtained. It is found that the elastic constants and the Debye temperature increase monotonically and the anisotropy is weakened with pressure. Moreover, the density of states (DOS) of NbB_2 at Fermi level under pressure decreased. The shift of positions of the sharp peaks near the Fermi level resulted from the charge transfer σ–π with pressure, which may indicate a decrease of the superconducting transition temperature T_c with pressure, in agreement with other theoretical results.

Acknowledgments

The authors would like to thank the Nature Science Fund of China Academy of Engineering Physics for support under

grant no 20060103 and the Fund of the Lab for Shockwave and Detonation Physics under grant nos 9140C6712010606 and 9140C6711010805, as well as the National Natural Science Foundation of China under grant nos 10776022 and 40606007.

References

[1] Nagamatsu J, Nakagawa N, Muranaka T, Zenitani Y and Akimitsu J 2001 *Nature* **410** 63
[2] Buzea C and Yamashita T 2001 *Supercond. Sci. Technol.* **14** R115
[3] Samsonov G V and Vinitskii I 1976 *Refractory Compounds* (Moscow: Metallurgia) (in Russian)
[4] Cooper A S, Corenzerst E, Longinotti L D, Matthias B T and Zachariasen W H 1970 *Proc. Natl Acad. Sci. USA* **67** 313
[5] Yamamoto A, Takao C, Masui T, Izumi M and Tajima S 2002 *Physica* C **383** 197
[6] Kotegawa H, Ishida K, Kitaoka Y, Muranaka T, Nakagawa N, Takagiwa H and Akimitsu J 2002 *Physica* C **378–381** 25
[7] Escamilla R, Lovera O, Akachi T, Duran A, Falconi R, Morales F and Escudero R 2004 *J. Phys.: Condens. Matter* **16** 5979
[8] Nunes C A, Kackzorowski D, Rogl P, Baldissera M R, Suzuki P A, Coelho G C, Grytsiv A, André G, Boureé F and Okada S 2003 *Acta Mater.* **53** 3679
[9] Takeya H, Togano K, Sung Y S, Mochiku T and Hirata K 2004 *Physica* C **408–410** 144
[10] Nunes C A, Kaczorowski D, Rogl P, Baldissera M R, Suzuki P A, Coelho G C, Grytsiv A, Andre G, Bouree F and Okada S 2005 *Acta Mater.* **53** 3679
[11] Islam A K M A, Sikder A S and Islam F N 2006 *Phys. Lett.* A **350** 288
[12] Sikder A S, Islam A K M A, Nuruzzaman M and Islam F N 2006 *Solid State Commun.* **137** 253
[13] Shein I R and Ivanovskii A L 2006 *Phys. Rev.* B **73** 144108
[14] Singh P P 2003 *Solid State Commun.* **125** 323
[15] Vajeeston P, Ravindran R, Ravi C and Ashokamani R 2001 *Phys. Rev.* B **63** 045115
[16] Heid R, Renker B, Schober H, Adelmann P, Ernst D and Bohnen K P 2003 *Phys. Rev.* B **67** 180510
[17] Wang H Y, Chen X R, Zhu W J and Cheng Y 2005 *Phys. Rev.* B **72** 172502
[18] Islam F N, Islam A K M A and Islam M N 2001 *J. Phys.: Condens. Matter* **13** 11661
[19] Vanderbilt D 1990 *Phys. Rev.* B **41** 7892
[20] Perdew J P and Wang Y 1992 *Phys. Rev.* B **45** 13244
[21] Payne M C, Teter M P, Allen D C, Arias T A and Joannopoulos J D 1992 *Rev. Mod. Phys.* **64** 1045
[22] Milman V, Winkler B, White J A, Packard C J, Payne M C, Akhmatskaya E V and Nobes R H 2000 *Int. J. Quantum Chem.* **77** 895
[23] Murnaghan F D 1994 *Proc. Natl Acad. Sci. USA* **30** 244
[24] Wang J, Yip S, Phillpot S R and Wolf D 1995 *Phys. Rev.* B **52** 12627
[25] Wallace D C 1972 *Thermodynamics of Crystals* (New York: Wiley)
[26] Karki B B, Ackland G J and Crain J 1997 *J. Phys.: Condens. Matter* **9** 8579
[27] Barron T H K and Klein M L 1965 *Proc. Phys. Soc.* **85** 523
[28] Mahmud S T, Islam A K M A and Islam M N 2004 *J. Phys.: Condens. Matter* **16** 2335
[29] Okamoto N L, Kusakari M, Tanaka K, Inui H, Yamaguchi M and Otani S 2002 *J. Appl. Phys.* **93** 88
[30] Spoor P S, Maynard J D, Pan M J, Green D J, Hellmann J R and Tanaka T 1997 *Appl. Phys. Lett.* **70** 1959
[31] Auld M A 1973 *Acoustic Fields and Waves in Solids* vol 1 (New York: Wiley)
[32] Steinle-Neumann G, Stixtude L and Cohen R E 1999 *Phys. Rev.* B **60** 791
[33] Anderson O L 1963 *J. Phys. Chem. Solids* **24** 909
[34] Schreiber E, Anderson O L and Soga N 1973 *Elastic Constants and their Measurements* (New York: McGraw-Hill)
[35] Ichitsubo T, Ogi H, Nishimura S, Seto T, Hirao M and Inui H 2002 *Phys. Rev.* B **66** 052514
[36] Bardeen J, Cooper L N and Schrieffer J R 1957 *Phys. Rev.* **108** 1175